Proc. Natl. Acad. Sci. USA
Vol. 91, pp. 6948–6952, July 1994
Biochemistry

Distinctive DNA conformation with enlarged major groove is found in Zn-finger–DNA and other protein–DNA complexes

LENA NEKLUDOVA AND CARL O. PABO

Howard Hughes Medical Institute and Department of Biology, Massachusetts Institute of Technology, Cambridge, MA 02139

Communicated by Stephen C. Harrison, April 6, 1994 (received for review September 21, 1993)

ABSTRACT **We have analyzed DNA conformations in a series of protein–DNA complexes, and we find that a distinctive conformation—with an enlarged major groove—occurs in a number of different complexes. During this analysis, we also developed a simplified model of DNA structure that illustrates the relative position of (*i*) the base pairs, (*ii*) the phosphate backbone, and (*iii*) the double-helical axis. This model highlights the key structural features of each duplex, facilitating the analysis and comparison of structures that are distinct from canonical A-DNA or B-DNA. Comparing DNA conformations in this way revealed that an otherwise unrelated set of protein–DNA complexes have interesting structural similarities, including an enlarged major groove. We refer to this class of structures as B_{eg}-DNA (where eg means enlarged groove). Since related features occur in such a diverse set of protein–DNA complexes, we suggest that this conformation may have a significant role in protein–DNA recognition.**

DNA conformation may play an important role in protein–DNA recognition and may help explain how proteins recognize specific sites on double-stranded DNA (for a recent review, see ref. 1). We have been particularly interested in understanding how DNA structures seen in protein–DNA complexes are related to the classical A-DNA and B-DNA structures. Several studies have suggested that Zn-finger binding sites may have a DNA conformation that is "intermediate" between A-DNA and B-DNA (2–4), and our recent crystallographic analysis of the GLI–DNA complex (5) supports this general idea. Seeing this unusual structure prompted us to analyze and compare the DNA sites in a set of protein–DNA complexes that have been solved at high resolution.

DNA structures usually are analyzed by determining parameters such as rise per base pair, helical pitch, groove widths, base-pair displacement, base-pair inclination, and sugar pucker (6). We started by calculating these "classical parameters" for each duplex, but we also developed a simplified model of DNA structure that helps us to see the key structural features and gives a clearer picture of the structural relationships. When represented with our model, DNA structures are classified by noting the spatial relationship of the base pairs, the phosphate backbone, and the double-helical axis.

We find unexpected similarities in DNA conformations in the GLI (5), trp (7), glucocorticoid (8), Zif268 (9), MetJ (10), engrailed (11), and Tramtrack (12) protein–DNA complexes. In these structures, the major groove is both deep (somewhat like A-DNA) and wide (like B-DNA), and we refer to this family of conformations as B_{eg}-DNA (where eg means enlarged groove). In studying other protein–DNA complexes, we find a range of conformations that are intermediate between B_{eg}-DNA and canonical B-DNA. This suggests that B-DNA can be smoothly deformed to give B_{eg}-DNA.

The publication costs of this article were defrayed in part by page charge payment. This article must therefore be hereby marked "*advertisement*" in accordance with 18 U.S.C. §1734 solely to indicate this fact.

METHODS

Our analysis of DNA structures involved the use of "classical parameters" (Table 1) and of a simplified model that we developed for this study. We have examined most of the protein–DNA complexes for which high-resolution structures were available, but we had to eliminate two complexes that are strongly bent [CAP (21) and E2 (22)] and we had to divide some other DNA fragments into several segments (Table 1). (The derivation of certain classical parameters and the use of our model require a relatively straight segment of DNA so that the helical axis is well defined.) Definition of classical parameters is based on the Cambridge convention (23) and further discussed in Table 1. Their values were computed using both the Dickerson NEWHELIX program (24) and our own set of routines. Since we have been interested in the global features of the DNA structures, parameters were averaged for each of the DNA segments.

During our analysis of these complexes, we also developed a three-dimensional model that used smoothed helices to represent the path of the DNA backbones and used rectangles to represent the averaged position of the base pairs (Fig. 1). Parameters for the two smoothed helices representing the DNA backbones are naturally defined by letting the radius equal R_P and the pitch equal that of the DNA. (R_P is the radius of a cylinder fit to all the phosphate atoms.) To describe the relative arrangement of these two smoothed helices (the two DNA backbones), it also is necessary to give a phase shift. [In a plane perpendicular to the double-helical axis, this would be the angle subtended by the minor grove, and this angle can be calculated from knowledge of the groove widths (Fig. 1).] Although base pairs are sketched as rectangles, it is the midline of the base pair that is the other key element in our model. This midline (a line segment connecting the C6 of the pyrimidine and the C8 of the purine) can be positioned by noting that: (*i*) The displacement and inclination of the midline correspond to the averaged displacement and inclination of the base pairs. (*ii*) In a Watson–Crick base pair, the length of the midline is ≈9.7 Å. (*iii*) The endpoints of this line segment (i.e., the C6 and C8 atoms) are essentially equidistant from the helices representing the DNA backbones. (The average difference in these distances was <0.25 Å in all but one of the DNA fragments that we examined.)

We also developed a type of simple planar sketch (Fig. 1) that summarizes the relative position of the base pair, the helical axis, and the two backbone strands. Roughly speaking, these sketches show a "cross section" of our full three-dimensional model. More precisely, the sketches are obtained as follows: we first project the C6–C8 line segment onto a plane that is perpendicular to the helical axis and then use the projected segment as the midline of a rectangle that represents a base pair. The projection of a line through N1 and N9 determines one side of this rectangle, and the width of the rectangle equals 2.6 Å. [We have verified that projections of the C1′–C1′, C6–C8, and N1–N9 line segments are

Abbreviation: eg (as subscript), enlarged groove.

Table 1. Parameters for DNA structures

DNA segment	Pitch, Å	Rise per bp	δ, no.			Groove width, Å		Incl, deg	Disp, Å	Rp, Å	D, Å
			A	B	Int	minor	major				
1. A-DNA (13)	34.6	2.88	15	0	1	10.1	8.2	13.6	−4.8	9.68	−3.76
2. A-DNA (14)	33.5	2.94	15	1	0	10.4	6.9	14.0	−4.1	9.36	−3.82
3. GLI (5)	36.0	3.07	8	8	2	7.4	12.5	9.3	−3.1	10.5	0.90
4. trp repressor (7)	33.1	3.13	2	13	3	7.0	10.6	9.2	−2.3	10.0	1.04
5. Glucocorticoid 1 (8)	35.0	3.24	3	11	4	7.4	11.4	10.5	−1.8	10.0	1.77
6. Zif268 (9)	36.5	3.25	0	15	5	8.2	11.5	9.5	−1.6	9.95	1.37
7. MetJ (10)	35.8	3.32	0	15	3	7.8	11.3	11.9	−1.5	9.8	1.90
8. Engrailed 1 (11)	33.6	3.19	2	15	5	7.5	10.2	10.8	−1.5	9.6	1.47
9. TTK (12)	33.9	3.23	0	12	5	6.8	11.2	8.7	−1.5	9.75	2.00
10. α2 (15)	34.6	3.33	19	16	5	6.6	11.7	7.3	−1.0	9.7	2.60
11. GCN4 (16)	34.0	3.28	0	34	0	6.3	11.7	4.5	−0.9	9.8	2.52
12. λ repressor 1 (17)	35.5	3.33	1	17	2	6.7	12.1	3.9	−0.9	9.7	2.31
13. 434 repressor 1 (18)	35.5	3.33	0	14	4	5.3	13.4	4.1	−0.6	9.7	3.89
14. Glucocorticoid 2 (8)	34.6	3.35	4	10	4	5.1	13.1	0.2	−0.5	9.6	3.47
15. 434 repressor 2 (18)	32.7	3.17	0	20	0	5.9	11.1	4.8	−0.4	9.7	3.05
16. λ repressor 2 (17)	35.0	3.35	0	18	2	7.1	11.4	6.7	−0.3	9.6	2.77
17. GAL4 (19)	34.1	3.30	0	20	0	5.9	11.8	5.1	0.0	9.3	3.59
18. Engrailed 2 (11)	36.9	3.54	1	15	4	6.0	13.2	1.8	−0.1	9.25	3.44
19. B-DNA (20)	33.2	3.31	3	16	5	4.8	12.3	−0.2	−0.1	9.3	3.58

Structural parameters for selected DNA duplexes. Lengths are given in ångstroms; angles are in degrees. Under δ torsion angles, we tabulate the number of angles of B-type (118° < δ < 180°) and the number of angles of A-type (50° < δ < 95°) (6). The number of δ angles between 95° and 118° is tabulated in the Int (intermediate) column. We compute major and minor groove widths by calculating distances between two best-fit helices through the phosphate atoms of the two DNA strands and then subtracting 5.8 Å to account for the van der Waals radii of the phosphate groups. For a DNA fragment making a nearly full helical turn, these groove widths agree well with the NEWHELIX values [for shorter segments, the standard definition of the groove widths (6) used by NEWHELIX is not applicable]. Inclination (Incl), computed for the base-pair centerline of C6–C8 with the NEWHELIX program, is approximately equal to the base-pair-plane inclination adopted by the Cambridge convention. Disp is displacement of the base-pair centerline (C6–C8) from the helical axis. *Rp* is the radius of the best-fit cylinder through all the phosphates. The parameter *D* is defined in Fig. 1. In our analysis, we split the DNA into shorter helical segments whenever the rms deviation of *P* atoms from the best-fit cylindrical surface exceeded 1 Å. When segmentation was necessary, we always attempted to use DNA segments that were contacted by individual domains or subunits of the protein. DNA segments used in this table had the following sequences (reading along one strand). Segments: 1, GGGATCCC; 2, GGGGCCCC; 3, TTGGGTGGT (bp 7–15); 4, GTACTAGTT (mol.2, bp 1–9); 5, GATGTTCTG (bp 10–18); 6, GCGTGGGCGT; 7, TAGACGTCT (bp 1–9); 8, TAATTACCTAA (bp 10–20); 9, TAAGGATA (bp 5–12); 10, CATGTAATTCATTTACACGC; 11, TCCTATGACTCATCCAG (bp 1–17); 12, GCGGTGATAT (bp 10–19); 13, AGTACAAAC (bp 1–9); 14, CAGAACATC (bp 1–9); 15, TTTCTTGTAT (bp 10–19); 16, ATACCACTGG (bp 1–10); 17, CCGGAGGACA (bp 1–10); 18, TTTGCCATGT (bp 1–10); 19, CGCGAATTCGCG. We list parameters for only one half-site of the trp- and GAL4–DNA complexes, because other half-sites are structurally similar. Tramtrack (TTK) parameters were averaged for the two similar copies of the complex present in the crystal (12).

nearly parallel (within 3° for all cases studied).] Points representing the sugar phosphate backbone are added to this sketch by (*i*) choosing the point on each phosphate helix that has the same height (measured along the helical axis) as the closest C6 or C8 atom and then (*ii*) projecting these points onto the same plane. After projecting onto this plane, the phosphate cylinder is drawn as a circle with radius R_P. (The center of this circle marks the position of the helical axis.) A smaller circle is centered on each of the two points that mark the position of phosphate helices, and the radius of these circles (2.9 Å) is intended to indicate the average radius of the sugar phosphate backbone.

This type of planar sketch makes the DNA structures easier to visualize. It accurately represents the key components of our three-dimensional model, including: approximate lengths of several important base-pair elements (midline, C1′–C1′, and N1–N9 segments), the displacements of these elements from the helical axis, the distances of the two phosphate helices from the midline endpoints, and the radius of the best-fit cylinder through the phosphates. This construction does not introduce serious distortions: in all the cases that we have studied, projection always changes these key components by <4%. [Distortions that occur during projection are determined by the cosines of various angles (such as the average values of the inclination and propeller twist), and these cosines were between 0.96 and 1 in all but one of the cases we have examined. For similar reasons, the dimensions of the rectangles representing the base pairs are nearly constant: deviations are within 2% for all DNA fragments studied.] Further details concerning the derivation and accuracy of the planar sketches are given in Fig. 1.

To summarize the connection between our model and the classical parameters, we note that all of the key features of our sketches are uniquely determined by three model parameters (Table 1). Two of these—R_P and displacement—are classical DNA structural parameters. *D* is a parameter we have introduced to characterize the relative displacement of (*i*) a line segment representing the base-pair midline and (*ii*) a line segment (not shown on the sketches) connecting the two points that mark the position of the two phosphate strands. (Note that *D* characterizes the relative position of the base pair and the backbone.) Analysis of our model shows that *D* can be expressed in terms of other classical parameters (see Fig. 1).

Although it is not used in this paper, we also have developed a model that incorporates *Y* displacement (24). In this model, the two phosphate strands are fit to two distinct (but coaxial) cylinders. This allows a more accurate model for some of the structures but does not significantly change the values of key components (mentioned above) and has little effect on the appearance of the planar sketches. In passing, we note that our model also allows us to estimate $R_{C1'}$, the radius of best-fit cylindrical surface through all C1′ atoms. $R_{C1'}$, which also is shown in our planar sketches, can be computed with an error of <0.3 Å from the base-pair displacement and the linear dimensions of the idealized base pair. This surface is interesting since it serves as a natural divider between the part of the model representing the base

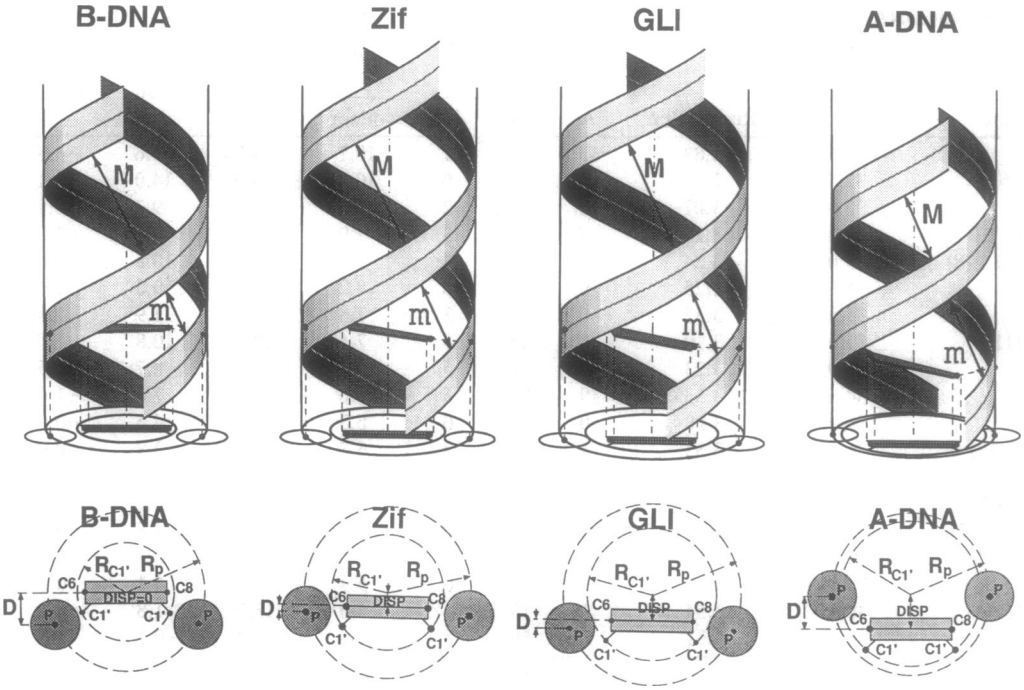

FIG. 1. Sketches illustrating a three-dimensional model and its two-dimensional "cross-section" for A-DNA (14), B-DNA (20), the Zif–DNA complex (9), and a segment of the GLI–DNA complex (5). In the sketches of the three-dimensional models (*Upper*), ribbons are used to represent the phosphate backbones. These are 5.8 Å wide (to approximate the van der Waals diameter of the phosphate group), and the ribbon midlines are the best-fit helices through the phosphates. Major and minor groove widths are denoted by M and m. In the planar models (*Lower*), base pairs are represented as rectangles parallel to C1′–C1′, with one side of the rectangle defined by the projection of the N1–N9 line and with a midline given by the projection of the C6–C8 line segment. [Note: in projection, the midline is nearly parallel (within 2° for all but one of the DNA segments studied) to the line connecting the centers of phosphate circles.] Relative displacement D can be expressed in terms of classical parameters as follows: $D = \text{Disp} + R_P \cdot \cos[(\text{Shift}/2) - \pi \cdot 9.7 \cdot \sin(\text{Incl})/\text{Pitch}]$, where 9.7 Å is the averaged length of base pair midline, Shift is the phase shift in radians across the minor groove, Disp is the displacement, and Incl is the inclination. The value of shift can be obtained from M and m by the approximate formula $\text{Shift}/(2\pi - \text{Shift}) = (\text{m} + 5.8)/(\text{M} + 5.8)$, which can be verified by "unwrapping" the cylindrical surface from the three-dimensional model. (The second term in the argument to cos is less significant and accounts for non-zero average inclination of base pairs.)

pairs and the part of the model representing the DNA backbone. It can be shown, based on purely geometric grounds, that knowing just the values of $R_{C1'}$ and R_P is sufficient to accurately estimate the base-pair displacement and to determine which of the grooves is wider. (Compared with the importance of $R_{C1'}$, inclination has a much smaller role in determining the displacement.)

RESULTS AND DISCUSSION

While trying to understand the role of DNA conformation in Zn finger–DNA recognition, we developed a simple model for DNA structure and discovered interesting features that occur in a diverse set of protein–DNA complexes. Our model provides a useful way of understanding how the DNA structures in the complexes are related to the canonical A-DNA and B-DNA conformations.

DNA structures usually are compared and classified by determining (*i*) the rise per base pair and the helical pitch, (*ii*) the width of the grooves, (*iii*) the inclination and displacement of the base pairs, (*iv*) the δ torsion angle (which is closely related to the sugar pucker), and (*v*) the radius R_P of the best fit cylindrical surface through the phosphates (6). Average values of these classical parameters were calculated for the GLI–DNA and Zif–DNA complexes. For comparison, we also calculated these parameters for A-DNA and B-DNA and for most of the protein–DNA complexes that have been solved at high resolution. (Examples are given in Table 1.)

Comparing these classical parameters shows that one region of the GLI DNA (where fingers 4 and 5 make specific base contacts) has values closer to those expected for A-DNA than those expected for B-DNA. Although they are not as pronounced, parameters for the Zif DNA also show some deviation from the values expected for classical B-DNA. [Our initial analysis of the Zif DNA (9) overlooked some unusual aspects of this structure. These were noted in a subsequent review (1) and also were mentioned in our report on the GLI Zn-finger–DNA complex (5).]

How can the unusual DNA conformations in the Zif and GLI complexes be described and classified? It has been proposed (2–4) that Zn finger–DNA complexes may have a structure intermediate between that expected for A-DNA and that expected for B-DNA. While this notion does convey some general impression about these structures, it cannot give a quantitative description. Conformational space is so complex that "distances" and "intermediate states" are not well defined: What would it mean for a structure to be x% A-DNA and (100 − x)% B-DNA? Studying Zif and GLI parameters (Table 1) illustrates the problems that occur if we try to describe these DNAs as a linear combination of A-DNA and B-DNA: Our description depends on which parameter we compare. For instance, the major groove of the GLI DNA is as wide as in B-DNA, whereas values of inclination are closer to those expected for A-DNA. GLI and Zif DNA actually have a larger helical radius (R_P) than seen in either canonical A-DNA or B-DNA. The sum of the major and minor groove widths also is larger for the GLI and Zif DNA than it is for A-DNA or B-DNA.

To provide a better tool for comparing these DNA structures, we developed a model that focuses on the relative position of the base pairs, the phosphate backbone, and the double-helical axis. [We thought this model might be useful since we had noted that parameters describing the base pairs (displacement and inclination) show some features of

A-DNA, and parameters describing the DNA backbone (δ angle and groove width) show more features characteristic of B-DNA.] As described in *Methods*, this model indicates the path of the two phosphate backbones with two smoothed helices and indicates the average position of the base pair with its midline segment (which connects the C8 of the purine to the C6 of the pyrimidine).

This three-dimensional model (Fig. 1) can readily be displayed on a graphics system and superimposed on the actual DNA coordinates, but we also developed a planar representation that captures the key features of the model. These planar sketches (Fig. 1) highlight similarities in the Zif and GLI DNA and illustrate how these differ from canonical A-DNA and B-DNA. In particular, the sketches show that the spatial relationship between the base pairs and the phosphate backbone is similar in the Zif and GLI DNA: the backbone is near the ends of the rectangle representing the base pair. This arrangement, which is distinct from the arrangements seen in A-DNA or B-DNA, gives a major groove that is both deep and wide. (The minor groove also remains fully accessible.)

Surprisingly, we find that a number of other protein–DNA complexes have DNA sites that resemble the Zif and GLI structures. This can be seen both from the parameter values (Table 1) and from sketches similar to those in Fig. 1. A similar conformation occurs in an 8-bp segment of the Tramtrack–DNA complex (12) that includes the Zn-finger binding site, but several other, unrelated complexes also have a DNA conformation closely resembling the Zif DNA. These include (*i*) trp complex (7), (*ii*) the half of the glucocorticoid complex that has nonspecific interactions (8), (*iii*) the MetJ complex (10), and (*iv*) the engrailed homeodomain–DNA complex (11) (Fig. 2). Many of these features had not been recognized or reported when the crystal structures were first published. (In some cases, e.g., for bent DNA, they may not have been noted because axis-dependent parameters cannot be reliably computed until the DNA is broken into appropriate segments.) The similarity of these structures suggests that this conformation is accessible to a variety of different sequences and suggests that it may play a significant role in protein–DNA recognition. Since the enlarged major groove is one of the important common features of these structures, we refer to this set of related structures as B_{eg}-DNA.

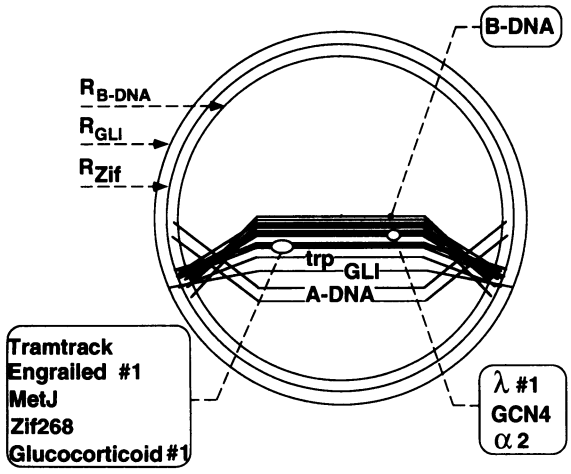

FIG. 2. Schematic representation of a larger set of DNA structures. This diagram is related to the planar sketches shown in Fig. 1, but each sketch has been streamlined so that more structures can be displayed. Here each structure is represented by (*i*) using one line segment to show the projected position of the C6–C8 midline and then (*ii*) connecting the ends of this line segment with the points representing the phosphate backbone. (Models are aligned by superimposing the points representing the helical axes and are oriented so that the C6–C8 line segments are parallel.) The diagram includes structures 1–14, 16, 18, and 19 from Table 1. (We omitted several B-like complexes to prevent the figure from becoming even more crowded.) A few structures are labeled individually, and we also indicate some clusters of structures that have similar displacements. Note that the order in which the base-pair midlines appear on this figure (from the bottom up) matches the order of DNA segments in Table 1 (from the top down).

B_{eg}-DNA has some similarities with B-DNA and some similarities with A-DNA, although the average classical parameters (Table 1) for the mentioned DNA segments (GLI is an exception) generally remain closer to those expected for canonical B-DNA. (The inclination, however, often has values closer to those expected for A-DNA.) On the whole, we think it is more useful to view B_{eg}-DNA as a distinct conformational class, rather than trying to describe it as an "intermediate" structure: There is no unique low-energy path in the conformational space between B-DNA and A-DNA, and no natural way to define how features should be mixed in an intermediate. Thinking of B_{eg}-DNA from this perspective also emphasizes the striking similarities between the Zif and GLI DNA and their differences from the canonical A-DNA and B-DNA structures.

Further studies will be needed to determine the full significance of this class of DNA conformations, but several observations seem especially relevant: (*i*) It is interesting that similar DNA conformations occur in an otherwise unrelated group of protein–DNA complexes that includes representatives from a number of different families of DNA-binding proteins. It appears that B_{eg}-DNA may provide a useful way of making the major groove more accessible for protein binding. (At this stage, we do not know whether these proteins recognize a distinctive conformation that exists in the free DNA or whether they induce this conformation as they bind.) (*ii*) It also is interesting that a large number of complexes have DNA conformations (Fig. 2) intermediate between that seen in the B_{eg}-DNA and that which occurs in canonical B-DNA. Intermediate structures are seen in the $\alpha 2$ complex (15), the GCN4 complex (16), and one-half of the λ complex (17). The fact that a range of intermediate structures occurs hints that B-DNA could be smoothly deformed to give B_{eg}-DNA. The glucocorticoid complex actually proves that the same DNA sequence can, under certain circumstances, adopt either conformation. One-half of the glucocorticoid complex (that with specific base contacts) has a relatively normal B-DNA structure, whereas the other half (that with nonspecific contacts) has a conformation very similar to that seen in the Zif complex. (*iii*) These distinctive structures are not correlated in any simple way with the sequence or composition of the binding sites (Table 1). Thus there is no overall preference for GC-rich sites, and the glucocorticoid DNA can—as mentioned above—adopt either conformation.

SUMMARY

Our analysis reveals a distinctive class of DNA conformations that occurs in a number of protein–DNA complexes. This class of conformations has an enlarged major groove and a characteristic relationship between the base pairs and backbone, and we refer to it as B_{eg}-DNA. The GLI DNA provides the most dramatic example, but related features clearly occur in the Zif complex and in other protein–DNA complexes. Known complexes with similar conformations include: (*i*) the Tramtrack complex (which contains two zinc fingers), (*ii*) the trp complex (which uses a helix–turn–helix unit for recognition and makes several water-mediated contacts with the bases), (*iii*) the glucocorticoid complex (where this structure appears in the half of the complex that makes nonspecific contacts with the bases), (*iv*) the engrailed homeodomain–DNA complex (which uses a helix–turn–helix unit to contact the major groove and an N-terminal arm to

contact the minor groove), and (ν) the MetJ complex (which uses an antiparallel β-sheet to make contacts in the major groove). Similar, but somewhat less pronounced, features appear in a number of other protein–DNA complexes. B_{eg}-DNA appears to be a distinct, relatively stable, and surprisingly common class of DNA conformations. It contains a set of otherwise unrelated protein–DNA complexes, and this suggests that it may play an important role in protein–DNA recognition.

Note Added in Proof. A recent paper by König and Richmond (25) reported the structure of a complex containing the GCN4-bZIP region and the ATF/CREB DNA site. From the thorough description given by the authors, it appears that this DNA fragment has the basic features of B_{eg}-DNA.

We thank Nikola Pavletich for his participation in the early stages of this work; Horace Drew and Aaron Klug for helpful comments on the Zif DNA structure; Daniela Rhodes for comments on the manuscript; and Paul Sigler for mentioning (after most of this analysis had been completed) the unusual DNA conformation in the trp complex. We also thank Tom Ellenberger, Ronen Marmorstein, Zbyszek Otwinowski, Paul Sigler, Tom Steitz, Simon Phillips, Weixin Xu, Rashmi Hegde, Louise Fairall, and Daniela Rhodes for sending coordinates of protein–DNA complexes. We thank Hani Tuval for help on graphics design. This research was supported by the Howard Hughes Medical Institute, by National Institutes of Health Grant GM-31471, and by equipment purchased with support from the PEW Charitable Trusts.

1. Travers, A. A. (1992) *Curr. Opin. Struct. Biol.* **2,** 71–77.
2. McCall, M., Brown, T., Hunter, W. N. & Kennard, O. (1986) *Nature (London)* **322,** 661–664.
3. Fairall, L., Martin, S. & Rhodes, D. (1989) *EMBO J.* **8,** 1809–1817.
4. Huber, P. W., Morii, T., Mei, H. -Y. & Barton, J. K. (1991) *Proc. Natl. Acad. Sci. USA* **88,** 10801–10805.
5. Pavletich, N. P. & Pabo, C. O. (1993) *Science* **261,** 1701–1707.
6. Saenger, W. (1984) *Principles of Nucleic Acid Structure* (Springer, New York).
7. Otwinowski, Z., Schevitz, R. W., Zhang, R. -G., Lawson, C. L., Joachimiak, A., Marmorstein, R. Q., Luigi, B. F. & Sigler, P. B. (1988) *Nature (London)* **335,** 321–329.
8. Luisi, B. F., Xu, W. X., Otwinowski, Z., Freedman, L. P., Yamamoto, K. R. & Sigler, P. B. (1991) *Nature (London)* **352,** 497–505.
9. Pavletich, N. P. & Pabo, C. O. (1991) *Science* **252,** 809–817.
10. Somers, W. S. & Phillips, S. E. V. (1992) *Nature (London)* **359,** 387–393.
11. Kissinger, C. R., Liu, B., Martin-Blanco, E., Kornberg, T. B. & Pabo, C. O. (1990) *Cell* **83,** 579–590.
12. Fairall, L., Schwabe, J. W. R., Chapman, L., Finch, J. T. & Rhodes, D. (1993) *Nature (London)* **366,** 483–487.
13. Lauble, H., Frank, R., Bloecker, H. & Heinemann, U. (1988) *Nucleic Acids Res.* **16,** 7799–7816.
14. McCall, M., Brown, T. & Kennard, O. (1985) *J. Mol. Biol.* **183,** 385–396.
15. Wolberger, C., Vershon, A. K., Liu, B., Johnson, A. D. & Pabo, C. O. (1991) *Cell* **67,** 517–528.
16. Ellenberger, T. E., Brandl, C. J., Struhl, K. & Harrison, S. C. (1992) *Cell* **71,** 1223–1237.
17. Beamer, L. J. & Pabo, C. O. (1992) *J. Mol. Biol.* **227,** 177–196.
18. Aggarwal, A. K., Rodgers, D. W., Drottar, M., Ptashne, M. & Harrison, S. C. (1988) *Science* **242,** 899–907.
19. Marmorstein, R., Carey, M., Ptashne, M. & Harrison, S. C. (1992) *Nature (London)* **65,** 408–414.
20. Drew, H. R., Wing, R. M., Takano, T., Broka, C., Tanaka, S., Itakura, K. & Dickerson, R. E. (1981) *Proc. Natl. Acad. Sci. USA* **78,** 2179–2183.
21. Schultz, S. C., Shields, G. C. & Steitz, T. A. (1991) *Science* **253,** 1001–1007.
22. Hedge, R. S., Grossman, S. R., Laimins, L. A. & Sigler, P. B. (1992) *Nature (London)* **359,** 505–512.
23. Dickerson, R. E., Bansal, M., Calladine, C. R., Diekmann, S., Hunter, W. N., Kennard, O., von Kitzing, E., Lavery, R., Nelson, H. C. M., Olson, W. K., Saenger, W., Shakked, Z., Sklenar, H., Soumpasis, D. M., Tung, C.-S., Wang, A. H.-J. & Zhurkin, V. B. (1989) *EMBO J.* **8,** 1–4.
24. Dickerson, R. E. NEWHELIX (Molecular Biology Institute, Univ. of California, Los Angeles), Version May 1989.
25. König, P. & Richmond, T. J. (1993) *J. Mol. Biol.* **233,** 139–154.